Science of Sintering, **49** (2017) 51-60

doi: 10.2298/SOS1701051L

UDK 546.824; 622.785

Two Step Sintering of $ZnTiO_3$ nanopowder

Nebojša Labus[1*)], Zorka Z. Vasiljević[1], Dana Vasiljević-Radović[2], Srđan Rakić[3], Maria V. Nikolić[4]

[1]Institute of Technical Sciences of SASA, Belgrade, Serbia

[2]Institute of Chemistry, Technology and Metallurgy, Department of Catalysis and Chemical Engineering, University of Belgrade, Belgrade, Serbia

[3]Institute of Physics, Faculty of Natural Sciences, University of Novi Sad, Novi Sad, Serbia

[4]Institute for Multidisciplinary Research, University of Belgrade, Belgrade, Serbia

Abstract:

Metastable nanopowder $ZnTiO_3$ was pressed into cylindrical compacts at 200 MPa. Compacts were treated by conventional heating with isothermal holding at 931 °C for 10 minutes, 25 minutes and 40 minutes. $ZnTiO_3$ compacts were also heated with a two-step sintering schedule with maximal 913 °C and isothermal holding at 896 °C, for approximately the same holding times as the isothermal schedule. Shrinkage during heating was monitored with a dilatometric device, while microstructure was determined with atomic force microscopy. XRD patterns were collected for the most interesting samples. Microstructures of sintered specimens showed differences introduced during the last sintering stage by the two different heating schedules. Goal of the presented work was to discuss the possible sintering mechanisms for the two step sintering schedulle according to the presented results.

Keywords: *Zinc titanate, Two-step sintering.*

1. Introduction

During sintering of compacted nanopowders, shrinkage measurements also indicate intensive sintering kinetic. Compared to micro powders, nanosized powders show more expressed onset and completion of the sintering process [1]. The origins of the peculiarities related with size phenomenon can be attributed to intensive rearranging processes of nanopowder particles at the onset, while at the final stage simultaneous grain impingement occurs due to numerous crystallization centers [2,3]. In this particular binary oxide combination of $ZnTiO_3$, the metastability of the main phase leads to the formation of spinel Zn_2TiO_4 and distortion of crystallites. This is somewhat surpassed by avoiding successive heating [4,5], but essential contribution to the preservation of the crystallite size is brought by the promptness of nanopowder sintering. Two-step sintering introduces the possibility to control grain growth [6,7]. The purpose of this work was observation of the influence of a two-step sintering schedule on $ZnTiO_3$ sintering, in view of crystallite size as well as grain size reduction and eventually phase composition favoring the metastable phase.

2. Experimental

$ZnTiO_3$ (Aldrich CAS [12036-43-0]) nanopowder with a 30 nanometer average

*) **Corresponding author**: nebojsa.labus@itn.sanu.ac.rs

particle size was used [8]. Compaction was carried out by a double sided uniaxial compaction method where no lubricant or binder was used. The applied pressure during the formation of specimens with a cylindrical shape 8 mm in diameter was 200 MPa, on a Hydraulic press RING, P-14, VEB THURINGER device. The average density of the compact was determined to be 2.6 10^3 kg/m^3. Shrinkage during the sintering process was monitored in a Bahr dilatometer 802 s device in air. The heating rate was 10 ^{o}C/min, isothermal holding at 931 ^{o}C for 10 minutes, 25 minutes and 40 minutes, while the two-step sintering schedule maximal 913 ^{o}C was followed by isothermal holding at 896 ^{o}C for overall holding times the same as the isothermal schedule. Isothermally heated specimens are denoted as G2, G4, and G6, non-isothermal is labeled as G1, and while two-step sintered specimens are G3, G5 and G7. The determined average density of sintered specimens was 4.3 10^3 kg/m^3. Atomic force microscopy (AFM) was performed on a Thermo microscopes autoprobe CP Research device in a contact mode with cantilever dimensions L=520 μm, W=40 μm, frequency f=20 kHz and spring constant k=0.9 N/m. Rough estimation of the grain size distribution was preformed from AFM images using more than a hundred measurements and the Semafore JEOL ver. 5.1 software [9]. X-ray diffraction measurements were performed on a Rigaku MiniFlex 600, U=40kV, I=15mA, wavelength CuKα, graphite monochromator, 2θ from 10^o to 100^o, step 0.02^o and holding time 4s. Structural refinement was carried out by the Rietveld method using the GSAS package [10] with the EXPGUI graphical user interface [11].

3. Results and discussion

Dilatograms were recorded to investigate the influence of isothermal and two step sintering schedules on shrinkage during the sintering process. The enlarged part of the sintering schedulle, presented on Fig.1, is shown in order to emphasize the temperature difference between isothermal and two-step sintering processes, noted as ΔT and declared as 35 ^{o}C. Also, the temperature difference of the step in the two step sintering process is declared as 17 ^{o}C. These values are found to be slightly small compared to other sources[6,7]. The sintering temperature of $ZnTiO_3$ must be lower than 945 ^{o}C. This is so because $ZnTiO_3$ as a metastable oxide transforms at that temperature to Zn_2TiO_4 and TiO_2. The importance of the powder particle size then lies in the fact that nanopowders require lower temperatures for sintering. The lower energy required for the sintering energy difference is obtained from the extreme curvatures that are relaxed during sintering. So the used small temperature differences thus strongly influence the process and are well suited for this particular system.

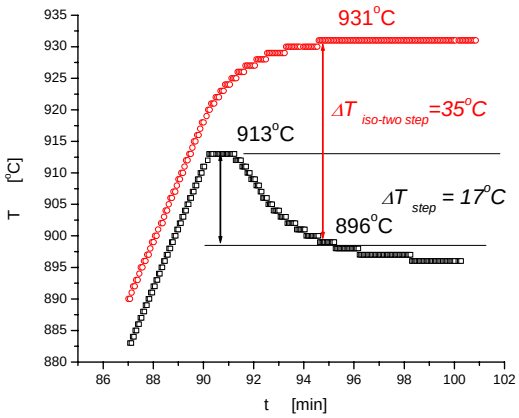

Fig. 1. Enlarged part of the temperature program schedules for two-step sintering and isothermal sintering.

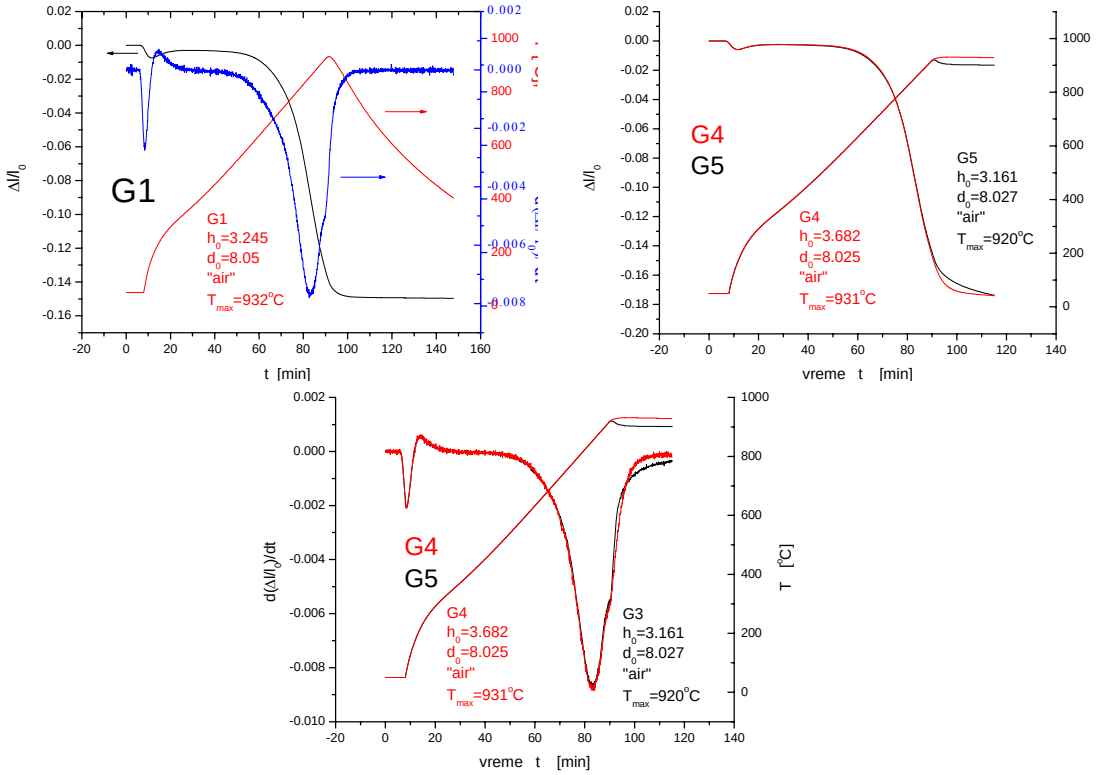

Fig. 2. Shrinkage and shrinkage rates with heating schedules for the compacts sintered isothermally and with a two-step sintering schedule. G1 non isothermally, G4, G5 - 25 miutes holding. Initial compact dimensions ,atmosphere and maximal temperature are given as the inset on every picture.

A dilatometer furnace was used for sintering and the holding time was changed from 0 minutes (G1 sintered non-isothermally), to 10 minutes (G2, G3), G4 and G5 sintered 25 minutes presented on Fig. 2, and G6, G7 sintered 40 minutes. The only influence of changing the heating schedule observed on shrinkage and shrinkage rate diagrams is in the final stage of sintering. During this stage, processes of grain growth and densification are competing, what becomes visible as a different behavior on the dimension - time diagram for the two schedules [12]. Two-step sintering has a slower kinetics. The sample sintered non-isothermally, G1, showed the same behavior during the cooling stage as an isothermally sintered sample with a sudden dimensional change. Since the two-step sintering process showed higher final shrinkages, and since they are proportional to densities, it is expected that the densification process is favored with slow kinetics. Such an obvious density change probably refers to closed porosity loss rather than grain growth.

Densities of the compacts, denoted as ρ_{press} on Fig. 3, illustrate the uniformity of the compaction procedure. The difference between particular compact densities is less than differences between sintered specimen densities. Densities of sintered samples, denoted as ρ_{sinter} on Fig. 3, showed that an isothermal holding period for longer isothermal holdings of 25 and 40 minutes resulted in lower densities than in the case of two-step sintering. This is simple evidence that a changed sintering schedule induces differences in sintered specimens. Previous investigations showed that air atmosphere does not favor closed porosity in sintered samples [13]. Although closed pores are not favored, they are still present. In this case since longer holding times result in a more pronounced density difference, it is expected that closing of pores is even more suppressed in the case of a two-step sintering process. The previously investigated nanopowder behavior showed a 2 % mass loss, explained as interacting of the oxide with atmosphere [13]. Mass gain resembles the greatest loss for

samples sintered for 25 minutes, but this loss is about 2 % and does not indicate a chemical reaction, or zinc volatilization, but rather reduction of the surface and adsorbed species proportional gain. The most obvious mass loss on Fig. 3 is present for samples G4 and G5.

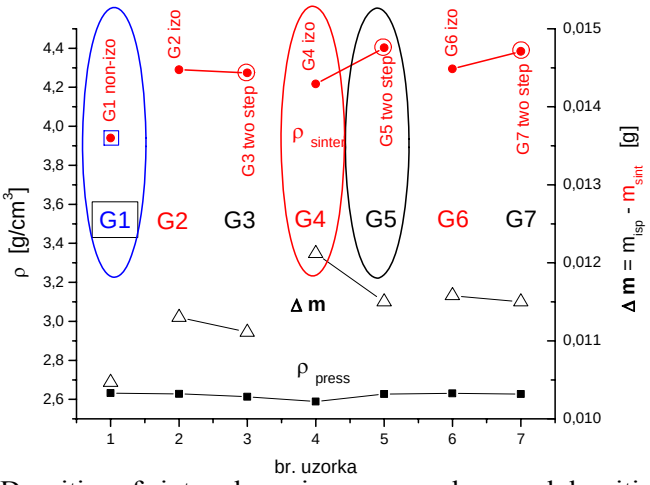

Fig. 3. Densities of sintered specimens, mass loss, and densities of compacts.

The most interesting and representative were G1 (sample sintered without isothermal holding), and G4 (sample sintered isothermaly for 25 minutes) and G5 (sample sintered with by two step sintering, holding time 25 minutes) were selected as the most interesting and representative for XRD analysis. Measured diffractograms of these samples are presented on Fig. 4. Fitting parameters were used as in previous work [4]. Three main phases were detected and their phase composition as well as crystallite size and lattice parameters are presented in Tab. I.

Tab. I Paramaters obtained by XRD refinement: phase compostion, crystallite size, and lattice parameters for G1, G4 and G5 samples.

Sample	Phase	Zn_2TiO_4	TiO_2 rutile	$ZnTiO_3$
G1	phase content %	64.96	16.61	18.43
	Crystallite size nm	141	112	188
	Cell parameters Å	*a*=8.45525(11)	*a*=4.5918(2) *c*=2.9597(3)	*a*=5.0777(2) *c*=13.9310(11)
G4	phase content wt.%	15.46	1.16	83.38
	Crystallite size nm	146	/	168
	Cell parameters Å	*a*=8.4608(2)	*a*=4.5926(4) *c*=2.9612 (5)	*a*=5.07989(10) *c*=13.9384(4)
G5	phase content %	13.19 wt.%	0.88	85.93
	Crystallite size nm	169	/	245
	Cell parameters Å	*a*=8.4557 (2)	*a*=4.5896 (5) *c*=2.9592 (6)	*a*=5.07606(11) *c*=13.9274 (5)

The phase composition shows interesting phase evolvement. Namely, the sample sintered without isothermal holding, G1, has the largest stable phase Zn_2TiO_4 content of 65 %. This suggests that non-isothermal heating favours formation of Zn_2TiO_4 and TiO_2. The percentage Zn_2TiO_4 in G4 and G5 samples is lower than in G1, and similar 15 % for G4 and 13 % for G5. Zinc metatitanate is regarded as a metastable phase and since non-isothermal heating induces a constant increase of vacancies and stress, it also hinders the formation of the metastbile phase [14,15].

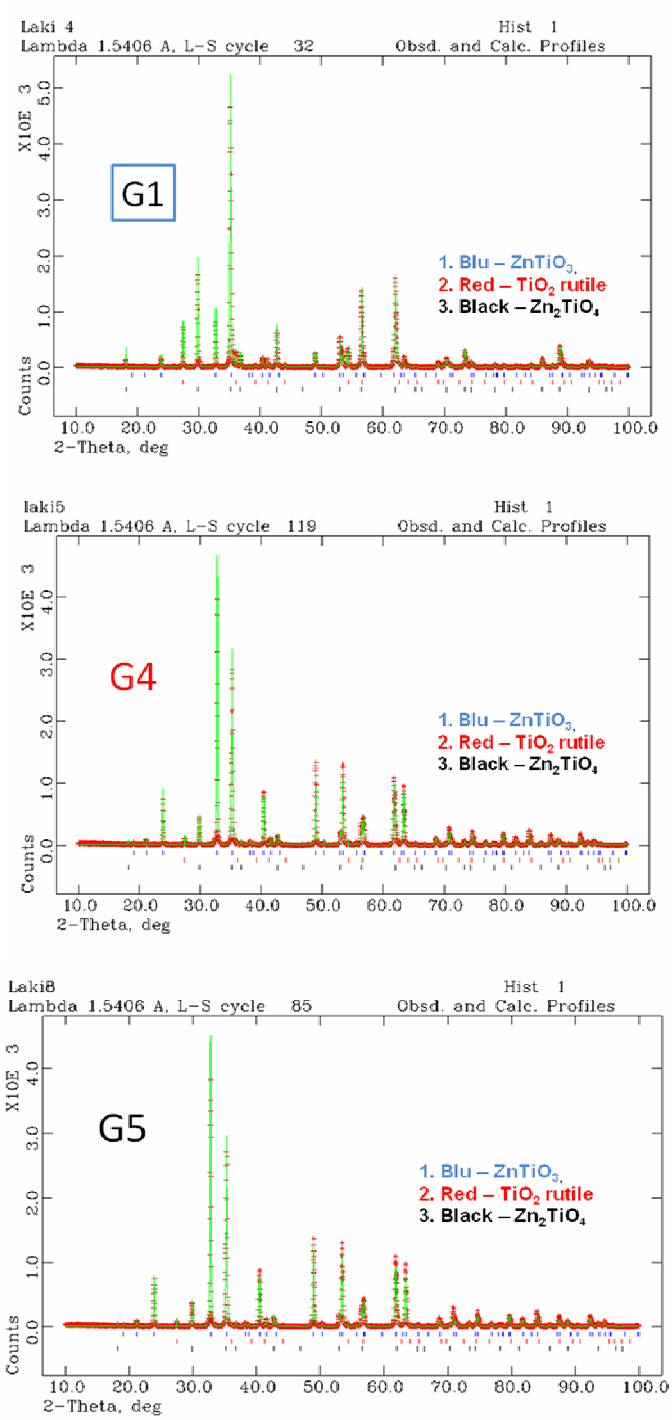

Fig. 4. XRD patterns with declared positions for each phase, G1 non isothermaly heated, G4 isothermally 25 minutes, G5 two-step sintering.

Larger crystallite sizes were obtained after two-step sintering of $ZnTiO_3$ (G5) compared to the isothermal G4 sample. The crystallite size is poorly affected by the heating schedule in the case of the Zn_2TiO_4 phase. For the Zn_2TiO_4 stable phase, a slightly larger crystallite size was obtained for two-step sintering. Titania, in rutile form, can not exceed 33 % of the Zn_2TiO_4 phase [16]. Increase in crystallite size for $ZnTiO_3$ to 245 nm size can be explained with the fact that the sudden temperature fall enhances recrystallization of $ZnTiO_3$.

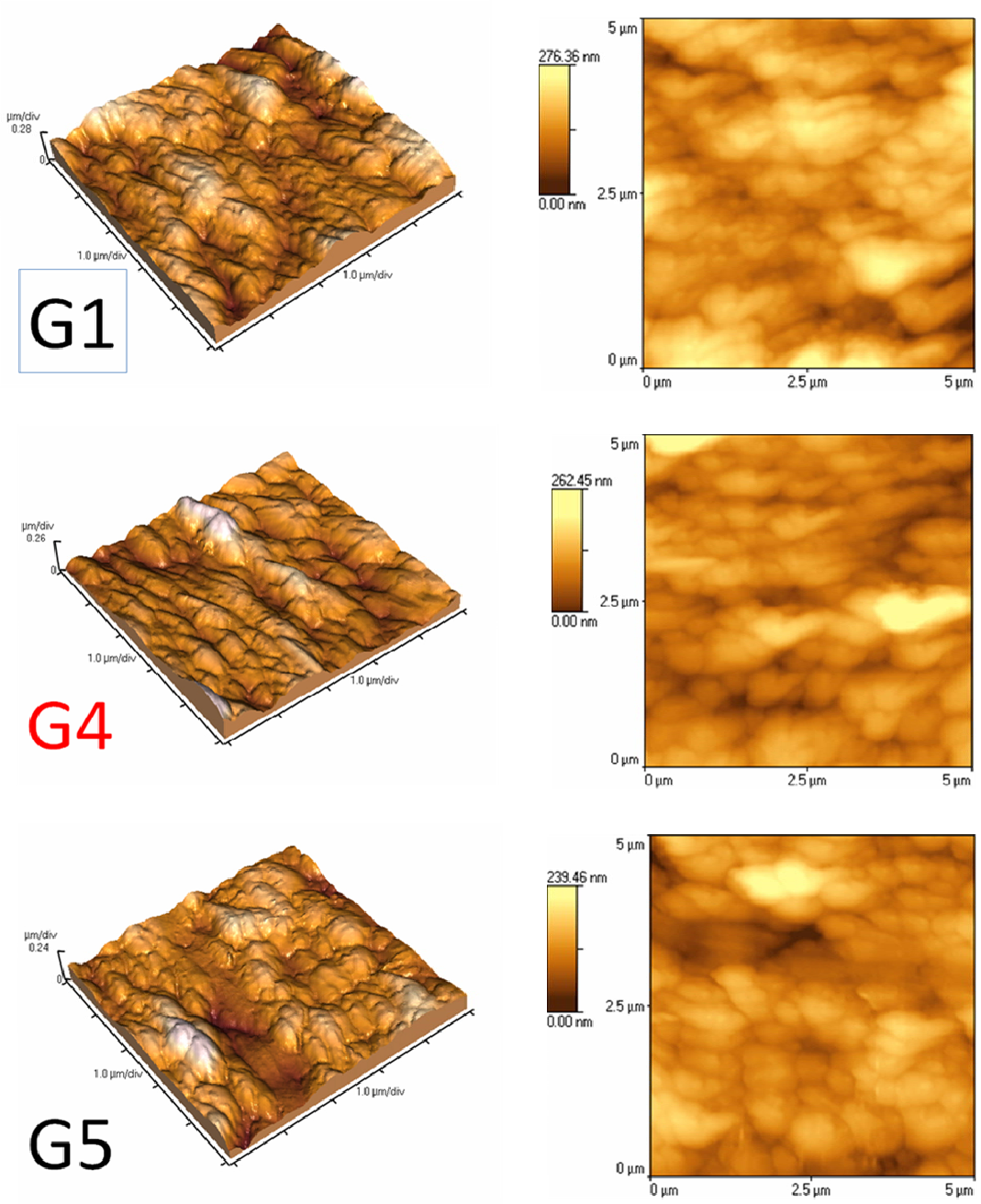

Fig. 5. AFM micrographies of G1 G4 and G5 samples represented in a three dimensional mode and planar view.

AFM micrographs of G1 G4 and G5 samples are shown in Fig. 5. Visible particles can be distinguished in the case of sample G1. Diameters estimated in previous work [8] for mean particle size was 30 nm. Here they can be recognized as texture points on the grain

structure. This structure strongly indicates that in the first stage of sintering of nanopowders, rearrangement takes place due to particle sliding. Nanopowder particles lose their characteristic spherical shape only after further densification during prolonged heating. The density achieved for non-isothermal sintering (sample G1) is lower than in the case of isothermally and two-step sintered samples (G4 and G5). This difference is due to interparticle pores and the sintering stage that is more advanced after isothermal holding.

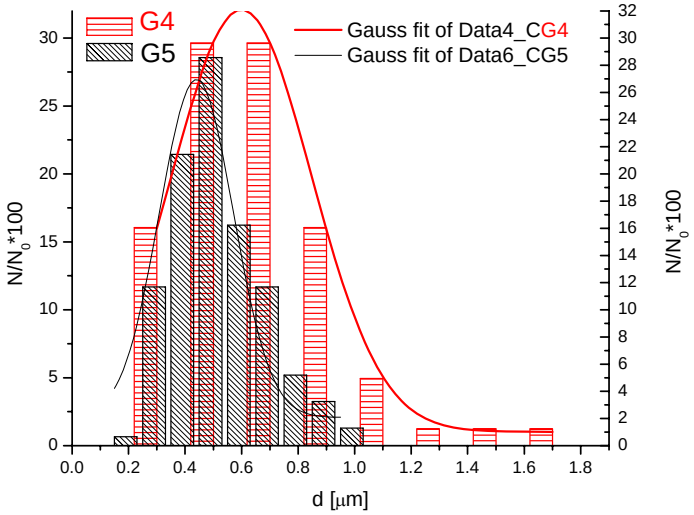

Fig. 6. Grain size distribution function for G4 and G5 samples.

The particle size distribution for G4 and G5 samples shown in Fig. 5 was determined and is presented on Fig. 6. It was performed on an unpolished surface, so the grain size determined is observed as a rude approximation, but it can fairly well represent changes in the grain size. It is obvious that, the mean grain size is lower and that the distribution is narrower for two-step sintering. Numerical data is given in Tab II. Relatively good fitting is achived with a Gaussian type of distribution. Statistics on the measured grain size values shows that the average mean value changes from 0.66 to 0.47 microns, while the standard deviation is almost halfed. Thus, with 25 minutes of isothermal holding, the G4 sample has grains that are not equal in size and also larger overall. In the case of the G5 sample the grains are more pronounced, equal in size and smaller as the result of the two step sintering mechanism.

Tab. II Fitting parameters for the grain size distribution function, Gaussian fit.

	Fitting procedure			Column statistics	
Sample	Chi^2/DoF ,R^2	Center	Width	Mean	sd((Y)Er±)
G4	0.06063 ,0.99977	0.59956	0.49567	0.66342	0.28367
G5	7.85207, 0.947	0.44001	0.26185	0.47596	0.16067

It is well accepted that sintering mechanisms encountered during the final sintering stage of nanopowders include superplasticity and grain rotation [6]. Beside these mechanisms it is evident that the number of vacancies linearly increases during nonisothermal heating. The step segment in two-step sintering can be read as a sudden lack of vacancies induced by cooling. This fact is in a contrast with the usual isothermal holding where the obtained number of vacancies is kept constant during the isothermal period, enabling intensive self-

diffusion. Also, in the case of an isothermal schedule, rapid reduction of the shrinking rate is observed, when an isothermal period is suddenly reached after a heating ramp. During this transition the defects created during the heating period would be annealed. In this case, a key parameter for describing the process would be the defect lifetime [17]. The grain growth behavior can be inhibited by vacancy production [18]. In that sense, the critical radius *Rc* can be regarded as a limiting stable grain size above which grain growth uninhibited by vacancies is possible. Obviously the critical grain size is temperature dependent. As the activation energies for grain boundary mobility and self-diffusion are generally different, the temperature variation of the critical grain size will depend on the interplay of the temperature dependencies of the mobility and the self-diffusion coefficient [19].

The following sequence of events is proposed: first during non-isothermal (linear) heating, the number of vacancies increases constantly. Diffusion forces vacancies generated at defects inside grains to reach the sink at grain boundaries. Sudden regression in heating, caused by a two-step sintering schedule at the chosen step temperature, induces a vacancy deficit inside the grain. After a retarding period when equilibrium is reached for the reduced number of vacancies, a lower number of vacancies are sent to the sinks. In our case the temperature step in the heating schedule is positioned after the maximum shrinkage rate. It is visible as sudden enhancement of the shrinkage rate, a sort of acceleration of shrinkage. This period is expected to belong to the nucleation period for the formation of new grains during recrystallization process. The process is also passing through the formation of nuclei with radiuses larger than the critical value and grain growth commences in a steadier path. At that moment a sudden temperature lowering brings the necessary cooling temperature difference and invokes the crystallization process, similar as in crystallization of glasses [20]. Grains are forming in an enhanced periodical structure recognizable in a larger domain of coherent scattering, namely the crystallite size. This is obvious from the different shrinkage paths, and narrow grain size distribution (Fig. 1 and Fig. 6).

At the same time high diffusion paths, namely grain boundaries, that were handling the excess of vacancies as sinks during the linear heating period, are now lowering their high diffusivity. At the same time, since the number of vacancies that are coming to the grain boundaries is reduced, their width is lowered. This process is also not distinguished instantly. The difference between the two schedules - two-step and isothermal, is not detected in shrinkage diagrams at the step moment. The curves look identical. But the difference appears after a while, since dilatation trajectories are now split. Then, finally, grain growth is suppressed since impingement of the favored recrystallized centers is now forming grains that are in contact thus forcing stress between individually relatively large grains that can`t grow now, using another mechanism such as grain rotation, Coble creep, or super plasticity, but only Nabbaro Herring diffusion creep [21]. This again leads to stable narrowing of the grain size distribution.

Presented results are mostly preliminary investigation of the phenomenon induced by two step sintering. They are confirming well known fact of the grain size reduction. They are also as well indicating possible sintering mechanisms responsible for the sintering of the metstabile ceramic nanopowder. Sintering phenomenon can be represented as a sequence of sintering mechanisms in a form of sintering diagram, but regarding the deformation map it is hard to attach particular mechanism to a particular temperature domain and strain rate. This is, along with better microstructure characterization, challenge for the next step experiments.

4. Conclusion

In this work we analyzed the impact of change in the sintering schedule to two-step sintering on grain size growth with the purpose of reducing it. In the case of the applied two-step sintering schedule grains exhibited a significant size reduction from 0.60 microns to 0.44

microns. They were also more pronounced and more equal in size. The determined crystallite size increased from 168 nm to 245 nm. Thus the recrystallization process was enhanced by the introduction of the temperature fall step in the two-step sintering schedule. The phase composition for a non-isothermally heated sample strongly favored Zn_2TiO_4 and TiO_2 as the more stable phases. Isothermal sintering and a two-step sintering schedule on the other hand improved the content of the perovskite $ZnTiO_3$ phase from 18 % to 85 %. Better observation of the grain size shape would answer the question of possible equilibrium reaching at a particular mean grain size and possible mechanism that is governing the grain size and shape.

Acknowledgement

This work was supported by the Ministry for Science, Education and Technological Development of the Republic of Serbia, project OI 172057. Also authors would like to express gratitude for useful advices to Miodrag Lukić about the two step sintering phenomenon.

5. References

1. N. Labus, S. Mentus, Z. Z. Đurić, M. V. Nikolić, Influence of Nitrogen and Air Atmosphere During Thermal Treatment on Micro and Nano Sized Powders and Sintered TiO_2 Specimens, Science of Sintering, 46 (2014) 365-375.
2. И. П. Арсентьева, М. М. Ристић, Ультрадисперсниые металлические порошки, ЦМС и ИТН САНУ, Београд 1987.
3. П. П. Будников, А. М. Гинстлинг, «Реакции в смесях твердых веществ», Строиздат, Москва, 1971.
4. $ZnTiO_3$ Pearson's Crystal Data. Dossier of: 1629506
5. N. Labus, J. Vujančević, M. V. Nikolić, Microstructure changes caused by thermal etching of sintered $ZnTiO_3$, PHYSICAL CHEMISTRY 2014, 12th International Conference onFundamental and Applied Aspects of Physical Chemistry, BELGRADE, 22-26 September 2014.
6. I. Wei Chen, X.-H. Wang, Sintering dense nanocrystalline ceramics without final stage grain growth, Nature, Vol. 404, 9 march 2000, 168-171.
7. Chin - Jen Wang, Chi - Yuen Huang, Yu - Chun Wu, Two step sintering of fine alumina - zirconia ceramics, Ceramics International, 35 (2009) 1467-1472.
8. N. Labus, J. Krstić, S. Marković, D. Vasiljević-Radović, M V. Nikolić, V. Pavlović , $ZnTiO_3$ Ceramic Nanopowder Microstructure Changes During Compaction, Science of Sintering, 45 (2013) 209-221.
9. SEMAFORE JEOL, digital slow scan image recording system, ver. 5.1., www.jeol.se
10. A. C. Larson, R. B. Von Dreele, General Structure Analysis System (GSAS), Los Alamos National Laboratory Report LAUR (2004) 86-748.
11. B. H. Toby, EXPGUI, a graphical user interface for GSAS, J. Appl. Cryst. 34 (2001) 210–213.
12. J. E. Burke, Role of Grain Boundaries in Sintering, Journal of the American Ceramic Society,Vol. 40, Issue 3, (1957) 80–85.
13. N. Labus, S. Mentus, S. Rakić, Z. Z. Đurić, J. Vujančević, M.V. Nikolić, Reheating of Zinc-titanate Sintered Specimens, Science of Sintering, 47 (2015) 71-81.
14. Y. Estrin, G. Gottstein, L. S. Schvindlerman, Thermodynamic effects on the kinetics of vacancy generating processes, Acta mater., Vol. 47, No. 13 (1999) 3541-3549.

15. J. J. Cleveland and R. C. Bradt, Grain size/microcracking relations for pseudobrookite oxides, J. Amer. Ceram. Soc., 61 (1978) 478-481.
16. Hyo Tae Ki, Yoonho Kim, Matjaz Valant, Danilo Suvorov, Titanium Incorporation in Zn_2TiO_4 Spinel Ceramics, J. Am. Ceram. Soc., 84 [5] (2001) 1081–86.
17. P. Roura, J. Costa, J. Farjas, Is sintering enhanced under non-isothermal conditions?, Materials Science and Engineering A337 (2002) 248-253.
18. Y. Estrin, G. Gottstein, E. Rabkin, L. S. Schvindlerman, On the kinetics of Grain Growth inhibited by vacancy generation, Scripta Materialia, 43 (2000) 141-147.
19. R. S. Averback, H. J. Hofler, H. Hahn and J. C. Logas, Sintering and Grain Growth in Nanocrystalline ceramics, NanoStructured Materials, Vol.1 (1992) 173-178.
20. C. N. R. Rao, K. J. Rao, Phase Transition in Solids, McGraw-Hill Inc., New York (1978).
21. T. H. Courtney, Mechanical Behavior of Materials, 2nd ed., McGraw-Hill, Boston, (2000).

Садржај: *Нанопрах метастабилног $ZnTiO_3$, испресован у цилиндричне испреске притиском од 200 MPa подвргнут је уобичајеном загревању са изотермским задржавањем на 931 °C у трајању од 10 минута, 25 минута и 40 минута. $ZnTiO_3$ испресци такође су загревани у режиму грејања за двостепено синтеровање са миксималних 913 °C и изотермским задржавањем на 896 °C, у трајању приближно истом као и за изотермско загревање. Скупљање током грејања праћено је дилатометром, док је микроструктура забележена микроскопијом атомске интеракције - АФМ. XRD дифрактограми су снимљени за најзначајније узорке. Микроструктура синтерованих узорака показала је разлике које су настале током последњег ступња синтеровања, услед два различита начина загревања.*
Кључне речи: *цинк-титанат, двостепено синтеровање.*